Published in final edited form as:
*Cancer Res*. 2011 April 1; 71(7): 2664–2674. doi:10.1158/0008-5472.CAN-10-3055.

# COX-2 blockade suppresses gliomagenesis by inhibiting myeloid-derived suppressor cells

**Mitsugu Fujita**[1,2], **Gary Kohanbash**[1,6], **Wendy Fellows-Mayle**[2], **Ronald L. Hamilton**[1,3], **Yoshihiro Komohara**[1,2], **Stacy A. Decker**[7], **John R. Ohlfest**[7], and **Hideho Okada**[1,2,4,5]

[1] Brain Tumor Program, University of Pittsburgh Cancer Institute, Pittsburgh, PA 15213

[2] Department of Neurological Surgery, University of Pittsburgh School of Medicine

[3] Department of Pathology, University of Pittsburgh School of Medicine

[4] Department of Surgery, University of Pittsburgh School of Medicine

[5] Department of Immunology, University of Pittsburgh School of Medicine

[6] Department of Infectious Diseases and Microbiology, University of Pittsburgh Graduate School of Public Health

[7] Department of Pediatrics, University of Minnesota, Minneapolis, MN 55455

## Abstract

Epidemiological studies have highlighted associations between the regular use of nonsteroidal anti-inflammatory drugs (NSAIDs) and reduced glioma risks in humans. Most NSAIDs function as cyclooxygenase-2 (COX-2) inhibitors that prevent production of prostaglandin $E_2$ ($PGE_2$). Since $PGE_2$ induces expansion of myeloid-derived suppressor cells (MDSCs), we hypothesized that COX-2 blockade would suppress gliomagenesis by inhibiting MDSC development and accumulation in the tumor microenvironment (TME). In mouse models of glioma, treatment with the COX-2 inhibitors acetylsalicylic acid (ASA) or celecoxib inhibited systemic $PGE_2$ production and delayed glioma development. ASA treatment also reduced the MDSC-attracting chemokine CCL2 in the TME along with numbers of $CD11b^{+}Ly6G^{hi}Ly6C^{lo}$ granulocytic MDSCs in both the bone marrow and TME. In support of this evidence that COX-2 blockade blocked systemic development of MDSCs and their CCL2-mediated accumulation in the TME, there were defects in these processes in glioma-bearing *Cox2*-deficient and *Ccl2*-deficient mice. Conversely, these mice or ASA-treated wild-type mice displayed enhanced expression of CXCL10 and infiltration of cytotoxic T lymphocytes (CTL) in the TME, consistent with a relief of MDSC-mediated immune suppression. Antibody-mediated depletion of MDSCs delayed glioma growth in association with an increase in CXCL10 and CTLs in the TME, underscoring a critical role for MDSCs in glioma development. Lastly, *Cxcl10*-deficient mice exhibited reduced CTL infiltration of tumors, establishing that CXCL10 limited this pathway of immune suppression. Taken together, our findings show that the COX-2 pathway promotes gliomagenesis by directly supporting systemic development of MDSC and their accumulation in the TME, where they limit CTL infiltration.

## Introduction

Gliomas are the most common primary malignant brain tumors and present with dismal patient prognosis. Despite the need for curative treatments, definitive information regarding

Corresponding: Hideho Okada, Suite G.12a, 5117 Centre Ave., Pittsburgh, PA 15213, Phone 412.623.1111/Fax 412.623.4747/ okadah@upmc.edu.

their etiology is lacking and identification of factors that influence the risk and prognosis remain undefined. Recent reports in epidemiology have exposed yet unexplained roles of immunosurveillance in gliomagenesis and survival of glioma patients. For example, the regular use of nonsteroidal anti-inflammatory drugs (NSAIDs) appears to be associated with reduced occurrence of malignant gliomas in humans (1,2). NSAIDs mediate their biological effects at least partially by suppression of cyclooxygenase (COX) 2 and its product prostaglandin (PG) $E_2$, which in turn induces differentiation of immunoregulatory cells, such as myeloid-derived suppressor cells (MDSCs) and regulatory T cells (Tregs), in tumor-bearing hosts (3–6).

MDSCs consist of two distinct populations, $Ly6G^{hi}Ly6C^{lo}$ granulocytic MDSCs (gMDSCs) and $Ly6G^{-}Ly6C^{hi}$ monocytic MDSCs (mMDSCs), and expand under pathological conditions including tumors (7). They negatively regulate both adaptive and innate immune responses by producing arginase-1, inducible nitric oxide synthase (iNOS; also known as NOS2), and reactive oxygen species (ROS) (7). Thus, MDSCs facilitate tumor progression by dampening immunosurveillance and are considered to be an important target for tumor immunotherapy. It is critical to gain a better understanding of the complex biological interactions between the immune system (MDSCs in particular) and developing gliomas.

In this regard, the chemokine CCL2 has been shown to play an important role in migration of MDSCs towards the tumor microenvironment (TME) (8). However, it is unknown whether the COX-2 pathway affects chemokine expression profiles that are responsible for MDSC accumulation in the TME.

In the current study, we evaluated our hypothesis that COX-2 blockade by NSAIDs would suppress gliomagenesis by inhibiting development of MDSCs and their accumulation in the TME using the *Sleeping Beauty* (*SB*) transposon-mediated *de novo* murine glioma model (9,10). Our findings in this study implicate significance of the COX-2 pathway in gliomagenesis through chemokine-mediated immune cell infiltration in the TME. Our data also suggest that NSAID-based prophylactic treatment strategies may provide therapeutic benefit for individuals at heightened risk of glioma development, assuming predictive risk factors can be identified.

## Materials and Methods

### Animals

Wild type (WT) C57BL/6 mice were obtained from Taconic Farms. C57BL/6-background mice deficient for the following genes were obtained from The Jackson Laboratory: *Cox-2*, *Ccl2*, and *Cxcl10*. Animals were bred and handled in the Animal Facility at the University of Pittsburgh per an Institutional Animal Care and Use Committee-approved protocol. As the *Cox-2*-deficient breeders were heterozygous, PCR using tail DNA was employed to genotype the mice per the vender's instruction.

### Intracelebroventricular DNA injection used for glioma induction

The procedure has been described previously (9). *In vivo*-compatible DNA transfection reagent (*In vivo*-JetPEI™) was obtained from Polyplus Transfection. The following DNA plasmids were used for glioma induction: pT2/C-Luc//PGK-SB13 (0.2 μg), pT/CAGGS-NRASV12 (0.4 μg), and pT2/shP53 (0.4 μg).

### Glioma cell culture

The procedure to establish glioma cell lines from *SB* transposon-mediated *de novo* murine gliomas has been described previously (10). The cultured cells were treated with the

following NSAIDs at the indicated concentrations: ASA (Sigma Aldorich), celecoxib (Biovision), or dimethylcelecoxib (kindly provided by Dr. Axel H. Schönthal, University of Southern California, CA). Cell proliferation assay using WST-1 (Roche) was performed on the indicated days per the manufacturer's instruction. The indicated groups were used as a control to determine the relative cell viability.

### $PGE_2$ release assay

The $PGE_2$ ELISA kit was obtained from R&D Systems. Assays were conducted per the manufacturer's instructions.

### *In vivo* NSAID treatment

We treated mice with ASA (10 mg/kg/day) or celecoxib (30 mg/kg/day) based on previous studies (11–14) and the U.S. Food and Drug Administration guidance (15). To treat neonates and unweaned mice with ASA, we prepared water-based solutions of 2 mg/ml ASA, and mice received the following volume of these solutions by oral gavage: 20 μl for the first week, 50 μl for the second week, and 100 μl for the third week after birth. When the mice were weaned on days 21 to 23 after birth, they started to receive the treatment via the following method: drinking water that contained 0.05 mg/ml ASAor diet that contained 150 ppm celecoxib.

### Quantitative real-time polymerase chain reaction (RT-PCR)

The procedure has been described previously (16). The following primers and probes were obtained from Applied Biosystems: *Ccl2* (Mm00441242_m1), *Cxcl10* (Mm99999072_m1), a n d *Nos2* (Mm01290688_m1).

### Isolation of brain-infiltrating leukocytes (BILs)

The procedure to isolate BILs has been described previously (17,18). Due to few numbers of BILs available from each individual, BILs were pooled from 3 mice in a given group for further evaluation. Fluorescent dye-conjugated antibodies for flow cytometry were obtained as follows: anti-CD4 (VH129.19), anti-CD8 (53–6.7), and anti-Ly6C (AL-21) from BD Biosciences; anti-CD11b (M1/70), anti-CD107a (1D4B), anti-FoxP3 (NRRF-30), and anti-Gr-1 (RB6-8C5) from eBioScience; anti-Ly6G (1A8) from BioLegend; anti-COX-2 (SP21) from AbCam. Flow data were obtained using a Coulter EPICS Cytometer (Beckman Coulter) and nalyzed using WinList software, version 6.0 (Verity Software House).

### Antibody-mediated $Gr1^+$ cell depletion assay

The procedure has been described previously (10). Anti-Gr-1 (RB6-8C5) monoclonal antibody (mAb) was obtained from eBioScience; control IgG was obtained from Sigma-Aldrich. Mice with developing gliomas received intraperitoneal (i.p.) injections of these Abs (0.25 mg/dose) on days 21, 23, 25, and 27 after plasmid DNA transfection.

### Statistical analyses

Student's t-test was performed to analyze differences between two groups; one-way analysis of variance with Holm's *post hoc* test was performed for multiple groups. Log-rank test was performed to analyze survival of mice with developing gliomas. All data were analyzed using R Environment, version 2.12.1. $P<0.05$ was considered to be statistically significant.

## Results

### Developing gliomas express COX-2

To address the effects of NSAID treatment on gliomagenesis, we first induced *de novo* gliomas in mice by intracerebroventricular transfection of *NRas* and small hairpin RNA against *P53* using the *SB* transposon system (9,10). By day 21 post-injection, the induced tumors demonstrated pathological characteristics of WHO grade 2 diffuse fibrillary astrocytoma seen in humans and progressed to WHO grade 3 anaplastic astrocytoma by day 60 (Supplementary Fig. S1). These findings suggest that these tumors initially develop as low-grade gliomas (LGGs) and progress to high-grade gliomas (HGGs), as often seen in the progression of human gliomas.

Subsequently, we evaluated COX-2 expressions in these mice (Supplementary Fig. S2). Glioma tissues, especially late-stage tumors (i.e. day 60) expressed COX-2 at high levels whereas adjacent normal brain tissues did not demonstrate detectable levels of COX-2 expression (Supplementary Fig. S2A, left). Moreover, $CD11b^+$ cells in the spleen and bone marrow consistently express COX-2 in the presence or absence of intracranial gliomas (Supplementary Fig. S2A, center and right, and S2B). These data suggest that the *de novo* gliomas express COX-2 whereas the tumors do not appear to enhance the baseline expression levels of COX-2 in the spleen or bone marrow.

### NSAID treatment inhibits glioma development *in vivo*

We then established primary glioma cell lines from these COX-2-positive tumors to evaluate the direct effects of COX-2 inhibitors on *in vitro* growth (Fig. 1A). ASA did not exhibit significant growth inhibitory effects on cultured glioma cells at up to 10 μM (= 1.8 mg/L culture medium; Fig. 1A, left). In contrast, celecoxib (center) and dimethylcelecoxib (right) inhibited glioma cell growth at similar concentrations, which is consistent with the reported direct cell-growth inhibitory effects of these agents (19). Concurrent with Supplementary Fig. S2, cultured glioma cells produced $PGE_2$ at high levels ($P<0.001$; Fig 1B). Moreover, both ASA and celecoxib significantly inhibited $PGE_2$ production from glioma cells at a concentration of 10 μM ($P<0.001$; Fig. 1B). These data suggest that ASA inhibits $PGE_2$ production from the glioma cells without affecting glioma cell growth while celecoxib inhibits both glioma cell growth and their $PGE_2$ production.

Next, we used ASA and celecoxib *in vivo* to treat mice with developing gliomas (Fig. 1C). With regard to the dose to administer, it has been reported that 20 to 50% of administered reagents remain active for 8 to 24 h in the blood circulation (20). Therefore, *in vivo* administration of ASA at 10 mg/kg/day in mice would exhibit a similar concentration in the body to that tested *in vitro* (1.8 mg/L). We also determined the dose of celecoxib to deliver *in vivo* (30 mg/kg/day in mice) that is equivalent to the clinical use (400 mg/day in human) (13,14). Daily 10 mg/kg ASA treatment initiated at the time of glioma induction significantly inhibited glioma development in WT mice with 3 of 8 treated mice surviving longer than 120 days ($P=0.0411$; Fig. 1C, left). In contrast, we observed no therapeutic effects when the treatment was initiated on day 21 (Fig. 1C, center), by which time solid gliomas were established (Supplementary Fig. S1B). However, 30 mg/kg celecoxib was effective in inhibition of glioma development even when the treatment was started on day 21 ($P=0.0269$; Fig. 1C, right), suggesting an involvement of its direct inhibitory effect on glioma cell growth (19).

We then addressed whether these treatments would reduce plasma $PGE_2$ levels in the mice with developing gliomas (Fig. 1D). The ASA treatment significantly reduced plasma $PGE_2$ levels in glioma-free mice ($P=0.012$; Fig. 1D, left). The mice with gliomas at days 50 to 60 exhibited higher plasma $PGE_2$ levels than those in the glioma-free mice ($P<0.001$), which

were reduced by the daily ASA treatment. The mice receiving the ASA treatment starting at day 0 demonstrated slightly reduced $PGE_2$ levels compared with the ones receiving treatment at day 21 ($P$=0.0457). As the tumor size was not significantly different between the ASA- vs. PBS-treated groups based on bioluminescence measurement (data not shown) (10), the observed reduction of $PGE_2$ levels is not likely due to merely smaller size of tumors in ASA-treated mice. Consistent with these data, the celecoxib treatment significantly reduced $PGE_2$ levels compared with the control treatment (P<0.001; Fig 1D, right). Taken together, these findings indicate that COX-2 blockade by NSAIDs may exert protective (rather than therapeutic) effects on gliomagenesis possibly through systemic $PGE_2$ inhibition. Based on the findings that pharmacological concentrations of celecoxib directly inhibit the proliferation of glioma cells (Fig. 1A), we thought that daily *in vivo* administration of ASA in mice with developing gliomas would reveal unique immune-mediated mechanisms operating *in vivo* without directly inhibiting the growth of glioma cells.

## The protective effect of ASA is concomitant with a decrease in systemic and tumor-infiltrating $CD11b^+Ly6G^+Ly6C^{lo}$ granulocytic MDSCs along with an increase in $CD107a^+$ CTLs

The results discussed in Fig. 1 led us to examine the immunological TME in response to the NSAID treatment. To this end, we extracted total RNA from brains, spleens, and bone marrows of the mice treated with ASA to evaluate the expression levels of *Ccl2* and *Cxcl10*; these chemokines are known to attract MDSCs (8,21) and activated T-cells (17,18), respectively. Glioma tissues exhibited high *Ccl2* expression levels, which were significantly suppressed when daily ASA treatment initiated on day 0 ($P$=0.0251; Fig. 2A, top left). In contrast, although *Ccl2* mRNA levels increased in the spleens and bone marrows of glioma-bearing mice compared with glioma-free mice, ASA treatment did not inhibit the *Ccl2* expressions in these organs (Fig. 2A, top center and right). Similar to the *Ccl2* expression profile, the mice with developing gliomas also exhibited higher expression levels of *Cxcl10* in the TME than those in the glioma-free mice ($P$<0.001; Fig. 2A, bottom left). The daily ASA treatment further enhanced the *Cxcl10* expression levels in the TME ($P$=0.0261). In contrast, we observed no alteration of *Cxcl10* expression levels in either the spleen or bone marrow in the presence or absence of the ASA treatment (bottom center and right).

Although the data described above suggest that the ASA treatment would affect MDSC accumulation in the TME, the COX-2 pathway is also known to promote systemic MDSC development in tumor-bearing mice (5). Therefore, we sought to evaluate the status of MDSCs in the organs tested above. The ASA-treated mice exhibited significant decreases in both frequencies and absolute numbers of $CD11b^+Ly6G^{hi}Ly6C^{lo}$ gMDSCs in the gliomas ($P$=0.032) and bone marrows ($P$=0.0199) when compared with the PBS-treated mice (Fig. 2B). In contrast, we observed no significant differences in $CD11b^+Ly6G^{lo}Ly6C^{hi}$ mMDSCs in these organs.

Since MDSCs are known to exert their biological effects by producing arginase-1 and iNOS (also known as NOS2) (7), we extracted total RNA from the sorted gMDSCs and mMDSCs to evaluate mRNA levels of these effector molecules (Fig. 2C). The ASA treatment significantly inhibited *Nos2* expressions in gMDSCs in all the organs tested (left). However, the treatment significantly inhibited the *Nos2* expression levels only in the glioma-infiltrating mMDSCs but not those in the other organs (P=0.050; right). We observed no effects in *Arg1* expression levels by the ASA treatment in any of the three sites (data not shown).

Consistent with the significant increase of *Cxcl10* observed in the TME (Fig. 2A, bottom left), the ASA-treated mice exhibited an increase in glioma-infiltrating $CD8^+$ T-cells

compared with the PBS-treated mice ($P$=0.020; Fig. 2D). Moreover, the $CD8^+$ T-cells in the ASA-treated mice demonstrated increased cell surface levels of a degranulation marker CD107a [mean fluorescence intensity (MFI) levels 9.8 vs 6.4] (22), suggesting improved effector functions of these cells compared with ones in PBS-treated mice.

### Deletion of *Cox-2* alleles leads to similar effects to those by the ASA treatment

The results discussed above led us to determine the specific roles of *Cox-2* gene in gliomagenesis. In particular, we directed our focus on the TME because we observed the most significant changes of both chemokine profiles as well as immune cell infiltrations in the brain. To this end, we induced *de novo* gliomas in *Cox-2*$^{+/+}$, *Cox-2*$^{+/-}$, and *Cox-2*$^{-/-}$ mice. The *Cox-2*$^{-/-}$ mice exhibited a delay in glioma development compared with the *Cox-2*$^{+/+}$ or *Cox-2*$^{+/-}$ mice ($P$<0.0478), with 5 of 6 *Cox-2*$^{-/-}$ mice surviving longer than 150 days (Fig. 3A). The *Cox-2*$^{+/-}$ mice also exhibited prolonged survival ($P$=0.0255), with 4 of 14 mice surviving longer than 150 days, compared with the *Cox-2*$^{+/+}$ mice, none of which survived longer than 119 days. Consistent with these data, plasma $PGE_2$ levels were significantly decreased in the *Cox-2*$^{+/-}$ mice compared with the *Cox-2*$^{+/+}$ mice ($P$<0.001), and the levels were further decreased in *Cox-2*$^{-/-}$ mice ($P$<0.001; Fig. 3B). When we evaluated the effects of *Cox-2* gene status on chemokine expressions in the TME, the *Cox-2*$^{-/-}$ mice exhibited lower levels of *Ccl2* ($P$≤0.016) and higher levels of *Cxcl10* ($P$≤0.0032) than the *Cox-2*$^{+/+}$ or *Cox-2*$^{+/-}$ mice (Fig. 3C). Consistent with this, the *Cox-2*$^{-/-}$ mice exhibited a decrease in glioma-infiltrating Gr-$1^+$ MDSCs ($P$=0.0016; Fig. 3D, top) with a concurrent increase in $CD8^+$ T-cells (P<0.001; bottom). Taken together, these data demonstrate that the glioma-bearing *Cox-2*$^{-/-}$ mice exhibit a similar phenotype to the ASA-treated mice and suggest that the ASA treatment exerts its main biological effects through suppression of the COX-2-$PGE_2$ pathway.

To determine whether altered *Cox-2* gene expression levels in glioma cells influenced their proliferation, we established glioma cell lines from glioma tissues obtained from the *Cox-2*$^{+/+}$ and *Cox-2*$^{+/-}$ mice. Although we were unable to establish *Cox-2*$^{-/-}$ glioma cells due to the lack of consistent tumor formation in these mice, *Cox-2*$^{+/+}$ and *Cox-2*$^{+/-}$ glioma cells proliferated at similar rates *in vitro* (Supplementary Fig. S3).

### Endogenous CCL2 promotes glioma development and tumor-infiltration of MDSCs

These data led us to hypothesize that the ASA treatment would induce dynamic changes in chemokine expression profiles in the TME, thereby reducing MDSCs and increasing CTLs. As CCL2 is known to be a primary chemokine that attracts MDSCs (8), we sought to evaluate direct impacts of CCL2 by inducing gliomas in *Ccl2*$^{-/-}$ mice. The *Ccl2*$^{-/-}$ mice exhibited a significant delay in glioma development with 3 of 10 mice surviving longer than 120 days ($P$=0.0188; Fig. 4A). In addition, the *Ccl2*$^{-/-}$ mice exhibited an increase in *Cxcl10* expression levels in the TME compared with WT mice ($P$=0.0347; Fig. 4B). When BILs were analyzed, the *Ccl2*$^{-/-}$ mice exhibited a decrease in Gr-$1^+$ MDSCs ($P$=0.0031; Fig. 4C, top) and an increase in $CD8^+$ T-cells ($P$=0.021; bottom) compared with WT mice. Taken together, these data suggest an important role of CCL2 in accumulation of not only MDSCs but also $CD8^+$ T-cells in the TME.

### mAb-mediated depletion of Gr-$1^+$ cells inhibits the glioma development

To gain a better understanding of the relationship between MDSCs and $CD8^+$ T-cell infiltration in the TME, we treated glioma-developing WT mice with anti-Gr-1 mAb to deplete Gr-$1^+$ MDSCs. Consistent with our previous data in type-1 interferon receptor-deficient mice (10), WT mice with developing gliomas that had received anti-Gr-1 mAb for systemic MDSC depletion exhibited a prolonged survival with 4 of 9 mice surviving longer than 120 days ($P$=0.0063; Fig. 5A). Furthermore, the mAb-treated mice exhibited an

increase in *Cxcl10* expression levels in the TME (P=0.0082; Fig. 5B), which was consistent with the observation in the *Ccl2*$^{-/-}$ mice (Fig. 4B). The mAb-treated mice exhibited a decrease in glioma-infiltrating Gr-1$^{+}$ MDSCs (*P*=0.014; Fig. 5C, top) as well as an increase in CD8$^{+}$ T-cells (*P*=0.023; bottom). Our combined results from COX-2 blockade, *Ccl2* deficiency, and MDSC depletion have uncovered a previously undescribed role of MDSCs in suppressing the expression of CXCL10, a critical chemokine for CD8$^{+}$ T-cell recruitment into the TME.

### Endogenous CXCL10 inhibits glioma development and promotes tumor-infiltration of CD8$^{+}$ T-cells

To address the specific roles of CXCL10 in gliomagenesis, we induced *de novo* gliomas in *Cxcl10*$^{-/-}$ mice. *Cxcl10*$^{-/-}$ mice with developing gliomas exhibited significantly shorter survival than WT mice (*P*=0.0171; Fig. 6A). The *Cxcl10*$^{-/-}$ mice also exhibited a decrease in CD8$^{+}$ T-cell infiltration (*P*=0.0079; Fig. 6B) and in their CD107a expression levels (MFI levels 9.5 vs 16.7), revealing a potential functional deficiency in addition to reduced numbers. Glioma-infiltrating CD8$^{+}$ T-cells in both the *Cxcl10*$^{-/-}$ and WT mice exhibited similar expression levels of CXCR3 (a receptor for CXCL10; Fig. 6C), which is consistent with previous reports demonstrating that CXCL10 in the TME rather than CXCR3 plays a predominant role in tumor-infiltration of CTLs (17,18). Collectively, the current study indicates important roles of the COX-2 pathway in gliomagenesis through systemic development of MDSCs and their CCL2-mediated accumulation in the TME along with a reduction of CXCL10-mediated tumor-infiltration of CTLs.

## Discussion

This is the first report documenting the immunological significance of the COX-2 pathway in gliomagenesis in mice. In the current study, treatment with ASA or celecoxib inhibited systemic $PGE_2$ production and delayed glioma development. This was especially true when the treatment was initiated shortly after the glioma-induction, suggesting significant involvement of the COX-2 pathway in the early stage of gliomagenesis. We also demonstrated a pivotal role of MDSCs and the MDSC-attracting chemokine CCL2 in the COX-2-mediated gliomagenesis.

The role of $PGE_2$ in MDSC development has been reviewed (23). In particular, *Ep2* (one of $PGE_2$ receptors)-deficient mice bearing 4T1 mammary carcinoma demonstrated a decrease of MDSC development and delayed tumor growth compared with WT mice (5). In the current study, we demonstrated for the first time that COX-2 blockade by NSAIDs as well as genetic deletion of *Cox-2* suppress glioma development in mice primarily by inhibiting MDSC accumulation in the TME (Figs. 1–3). We also observed a negative correlation between MDSCs and degranulating (CD107a$^{+}$) CD8$^{+}$ T-cells in the TME (Figs. 4C and 5C), suggesting that MDSCs suppress the effector function of CD8$^{+}$ T-cells in the TME and thereby facilitate glioma progression.

Although the ASA treatment inhibited systemic $PGE_2$ levels regardless of the timing to be initiated, it did not provide any therapeutic benefit when it was initiated after the tumor had already been established (Fig. 1 and Supplementary Fig. S1). Similarly, while homozygous *Cox-2*$^{-/-}$ mice demonstrated remarkably prolonged survival compared with *Cox-2*$^{+/+}$ mice (*P*<0.0478), heterozygous *Cox-2*$^{+/-}$ mice demonstrated only modest, albeit significant, prolongation of survival and reduction in plasma $PGE_2$ levels compared with *Cox-2*$^{+/+}$ mice (Fig. 3A and 3B). Furthermore, the heterozygous *Cox-2*$^{+/-}$ mice did not demonstrate significant differences in chemokine expressions and BIL profiles compared with *Cox-2*$^{+/+}$ mice (Fig. 3C and 3D). These data, together with remarkable suppression of $PGE_2$ levels by the ASA treatment (Fig. 1B), imply that a substantial threshold of $PGE_2$ suppression has to

be achieved to observe the clinical benefit of this strategy. These observations also suggest that ASA administration in humans might be only beneficial in prophylactic settings but not in patients with clinically diagnosed gliomas. Consistent with our interpretation, a recent study has demonstrated that long-term use of ASA reduces cancer risks in human (24).

With regard to the effects of ASA on each of the two distinct MDSC populations ($Ly6G^{hi}Ly6C^{lo}$ gMDSCs and $Ly6G^{-}Ly6C^{hi}$ mMDSCs), the ASA treatment preferentially reduced gMDSCs than mMDSCs in the organs tested (Fig. 2B). Taken together with a previous study demonstrating that under inflammatory conditions, expansion of gMDSCs occurs at a greater degree than that of mMDSCs (25), gMDSCs may be more susceptible than mMDSCs to $PGE_2$-mediated expansion and NSAID-mediated suppression. With regard to their functional differences, several studies have collectively indicated that gMDSCs preferentially express arginase-1 through the STAT3 signaling whereas mMDSCs express iNOS through the STAT1 signaling (7). Of interest, this proposed paradigm contrasts to our data demonstrating that gMDSCs also express iNOS that can be inhibited by ASA (Fig. 2C). Therefore, it is possible that our observations are unique to gliomas. Further studies are warranted to elucidate the mechanisms underlying the suppressive effects of each of MDSC populations in both human and mouse cancers located in a variety of organs.

CCL2 is known to be one of the primary chemokines attracting MDSCs towards TME (8), which is consistent with our observation that genetic depletion of *Ccl2* induced a significant decrease in MDSC accumulation in the TME (Fig. 4). In detail, both gMDSCs and mMDSCs express the receptor CCR2 although its expression levels have been shown to be higher on mMDSCs than gMDSCs (26), suggesting that the CCL2-CCR2 chemokine-receptor axis can mediate the migration of both gMDSCs and mMDSCs.

Simultaneously, our data showed that CCL2 blockade (and resulting inhibition of MDSCs) led to increases of *Cxcl10* expression and $CD8^{+}$ T-cell infiltration in the TME (Figs. 4 and 5). This contrasts to a previous study demonstrating that CCL2 mediates accumulation of activated T-cells in a glioma xenograft (27). We think that this difference reflects the immunocompetent status of mice in our spontaneous tumor model versus the xenograft model that requires immune deficient hosts. Given that CCR2, a cognate receptor for CCL2, is expressed in a wide range of immune cells including monocytes, MDSCs, Tregs, and effector T-cells (28), the CCL2-CCR2 axis operates in all cell populations that express the ligand CCL2 and/or the receptor CCR2 in our syngeneic glioma model. However, CCL2 in the TME is likely to recruit primarily MDSCs (8). Then, MDSCs inhibit the type-1 functions of DCs (29,30), including DC production of CXCL10 (18,31). Taken together, we propose that CCL2-attracted MDSCs inhibit CXCL10 production in the TME through suppression of DCs.

COX-2 and $PGE_2$ promote *de novo* induction of Tregs (32). Consistent with this, the ASA treatment inhibited Treg accumulation in the TME in our model (Supplementary Fig. S4). In this regard, we have previously attempted to address a role of Tregs in gliomagenesis by mAb-mediated depletion (10) and observed no significant effects of Treg-depletion on glioma development. Therefore, we rather focused on the roles of MDSCs in the current study. To elucidate a role of Tregs further, we are currently incorporating a Treg-attracting chemokine CCL22 in the *SB*-mediated glioma induction system; this system will allow us to address specific effects of CCL22 in the TME and glioma-infiltrating Tregs attracted by CCL22. Furthermore, it has been shown that glioma cell-derived CCL2 promotes Treg migration (33). We will elucidate the impact of these chemokines on Treg development and accumulation in future studies.

Collectively, the findings in the current study reveal the important roles of the COX-2 pathway in gliomagenesis through an increase in MDSC development and accumulation as well as a decrease in CXCL10-mediated $CD8^+$ T-cell infiltration in the TME. The data also support development of immunoprevention strategies that could be implemented in people with an increased risk for glioma development. To this end, it will be critical to gain a better understanding of the etiology and risk factors for glioma development in humans. Although risk factors for gliomas are still largely unknown, patients with LGGs are known to be at extremely high risks for developing HGGs (34). Based on our data demonstrating that early-stage gliomas on day 21 resemble human LGGs (Supplementary Fig. S1) and that celecoxib treatment starting on day 21 is effective (Fig. 1B), patients with LGGs may benefit from celecoxib treatment to reduce the risk for malignant progression with HGGs.

With regard to novel risk factors for glioma, we recently reported that single-nucleotide polymorphisms (SNPs) in *IFNAR1* and *IFNA8* correlate with altered overall survival of patients with WHO grade 2–3 gliomas (10). Others have reported that SNPs in *IL-4R* and *CX3CR1* correlate with survival of glioma patients (35–38). Although these data do not directly dictate risk factors for glioma development, it might be helpful to reveal functional significance of these SNPs in order to identify individuals who have a risk of gliomas and are likely to benefit from future clinical trials with NSAID-based immunoprevention. Based on the current study, future studies evaluating SNPs in *Cox-2, Ccl2 as well as Cxcl10* in relation to glioma risks and prognosis are warranted.

## Supplementary Material

Refer to Web version on PubMed Central for supplementary material.

## Acknowledgments

**Financial Support**

This work was supported by the following grants: the National Institute of Health 1R01NS055140 (HO), 2P01NS40923 (HO), 1P01CA132714 (HO), and 1R21NS055738 (JRO); American Cancer Society RSG-09-189-01-LIB (JRO); Pittsburgh Foundation D2008-0433 (MF); the Cancer Center Support Grant P3CA047904 (UPCI).

We appreciate Dr. Axel H. Schönthal for providing us with demethylcelecoxib. We also thank Heather A. McDonald, Louis Delamarre, and Tara E. Hymes for their technical assistance.

## References

1. Scheurer ME, El-Zein R, Thompson PA, et al. Long-term anti-inflammatory and antihistamine medication use and adult glioma risk. Cancer Epidemiol Biomarkers Prev. 2008; 17:1277–81. [PubMed: 18483351]
2. Sivak-Sears NR, Schwartzbaum JA, Miike R, Moghadassi M, Wrensch M. Case-control study of use of nonsteroidal antiinflammatory drugs and glioblastoma multiforme. Am J Epidemiol. 2004; 159:1131–9. [PubMed: 15191930]
3. Rodriguez PC, Hernandez CP, Quiceno D, et al. Arginase I in myeloid suppressor cells is induced by COX-2 in lung carcinoma. J Exp Med. 2005; 202:931–9. [PubMed: 16186186]
4. Ochoa AC, Zea AH, Hernandez C, Rodriguez PC. Arginase, prostaglandins, and myeloid-derived suppressor cells in renal cell carcinoma. Clin Cancer Res. 2007; 13:721s–6s. [PubMed: 17255300]
5. Sinha P, Clements VK, Fulton AM, Ostrand-Rosenberg S. Prostaglandin E2 promotes tumor progression by inducing myeloid-derived suppressor cells. Cancer Res. 2007; 67:4507–13. [PubMed: 17483367]
6. Wang D, Dubois RN. Eicosanoids and cancer. Nat Rev Cancer. 2010; 10:181–93. [PubMed: 20168319]

7. Gabrilovich DI, Nagaraj S. Myeloid-derived suppressor cells as regulators of the immune system. Nat Rev Immunol. 2009; 9:162–74. [PubMed: 19197294]
8. Huang B, Lei Z, Zhao J, et al. CCL2/CCR2 pathway mediates recruitment of myeloid suppressor cells to cancers. Cancer Lett. 2007; 252:86–92. [PubMed: 17257744]
9. Wiesner SM, Decker SA, Larson JD, et al. De novo induction of genetically engineered brain tumors in mice using plasmid DNA. Cancer Res. 2009; 69:431–9. [PubMed: 19147555]
10. Fujita M, Scheurer ME, Decker SA, et al. Role of type 1 IFNs in antiglioma immunosurveillance--using mouse studies to guide examination of novel prognostic markers in humans. Clin Cancer Res. 2010; 16:3409–19. [PubMed: 20472682]
11. Yoshida S, Amano H, Hayashi I, et al. COX-2/VEGF-dependent facilitation of tumor-associated angiogenesis and tumor growth in vivo. Lab Invest. 2003; 83:1385–94. [PubMed: 14563940]
12. Miliaras S, Miliaras D, Vrettou E, Zavitsanakis A, Kiskinis D. The effect of aspirin and high fibre diet on colorectal carcinoma: a comparative experimental study. Tech Coloproctol. 2004; 8(Suppl 1):s59–61. [PubMed: 15655645]
13. Jimeno A, Amador ML, Kulesza P, et al. Assessment of celecoxib pharmacodynamics in pancreatic cancer. Mol Cancer Ther. 2006; 5:3240–7. [PubMed: 17172427]
14. Park W, Oh YT, Han JH, Pyo H. Antitumor enhancement of celecoxib, a selective Cyclooxygenase-2 inhibitor, in a Lewis lung carcinoma expressing Cyclooxygenase-2. J Exp Clin Cancer Res. 2008; 27:66. [PubMed: 19000324]
15. U.S. Food and Drug Administration. Guidance for Industry: Estimating the Maximum Safe Starting Dose in Initial Clinical Trials for Therapeutics in Adult Healthy Volunteers. FDA; 2005.
16. Muthuswamy R, Urban J, Lee JJ, Reinhart TA, Bartlett D, Kalinski P. Ability of mature dendritic cells to interact with regulatory T cells is imprinted during maturation. Cancer Res. 2008; 68:5972–8. [PubMed: 18632653]
17. Fujita M, Zhu X, Sasaki K, et al. Inhibition of STAT3 promotes the efficacy of adoptive transfer therapy using type-1 CTLs by modulation of the immunological microenvironment in a murine intracranial glioma. J Immunol. 2008; 180:2089–98. [PubMed: 18250414]
18. Fujita M, Zhu X, Ueda R, et al. Effective immunotherapy against murine gliomas using type 1 polarizing dendritic cells--significant roles of CXCL10. Cancer Res. 2009; 69:1587–95. [PubMed: 19190335]
19. Schonthal AH, Chen TC, Hofman FM, Louie SG, Petasis NA. Celecoxib analogs that lack COX-2 inhibitory function: preclinical development of novel anticancer drugs. Expert Opin Investig Drugs. 2008; 17:197–208.
20. Levy G, Tsuchiya T. Salicylate accumulation kinetics in man. N Engl J Med. 1972; 287:430–2. [PubMed: 5044917]
21. Dzenko KA, Song L, Ge S, Kuziel WA, Pachter JS. CCR2 expression by brain microvascular endothelial cells is critical for macrophage transendothelial migration in response to CCL2. Microvasc Res. 2005; 70:53–64. [PubMed: 15927208]
22. Mathew A, Terajima M, West K, et al. Identification of murine poxvirus-specific CD8+ CTL epitopes with distinct functional profiles. J Immunol. 2005; 174:2212–9. [PubMed: 15699154]
23. Ostrand-Rosenberg S, Sinha P. Myeloid-derived suppressor cells: linking inflammation and cancer. J Immunol. 2009; 182:4499–506. [PubMed: 19342621]
24. Rothwell PM, Fowkes FG, Belch JF, Ogawa H, Warlow CP, Meade TW. Effect of daily aspirin on long-term risk of death due to cancer: analysis of individual patient data from randomised trials. Lancet. 2010; 377:31–41. [PubMed: 21144578]
25. Youn JI, Nagaraj S, Collazo M, Gabrilovich DI. Subsets of myeloid-derived suppressor cells in tumor-bearing mice. J Immunol. 2008; 181:5791–802. [PubMed: 18832739]
26. Movahedi K, Guilliams M, Van den Bossche J, et al. Identification of discrete tumor-induced myeloid-derived suppressor cell subpopulations with distinct T cell-suppressive activity. Blood. 2008; 111:4233–44. [PubMed: 18272812]
27. Brown CE, Vishwanath RP, Aguilar B, et al. Tumor-derived chemokine MCP-1/CCL2 is sufficient for mediating tumor tropism of adoptively transferred T cells. J Immunol. 2007; 179:3332–41. [PubMed: 17709550]

28. Deshmane SL, Kremlev S, Amini S, Sawaya BE. Monocyte chemoattractant protein-1 (MCP-1): an overview. J Interferon Cytokine Res. 2009; 29:313–26. [PubMed: 19441883]

29. Mantovani A, Sica A, Allavena P, Garlanda C, Locati M. Tumor-associated macrophages and the related myeloid-derived suppressor cells as a paradigm of the diversity of macrophage activation. Hum Immunol. 2009; 70:325–30. [PubMed: 19236898]

30. Greifenberg V, Ribechini E, Rossner S, Lutz MB. Myeloid-derived suppressor cell activation by combined LPS and IFN-gamma treatment impairs DC development. Eur J Immunol. 2009; 39:2865–76. [PubMed: 19637228]

31. Padovan E, Spagnoli GC, Ferrantini M, Heberer M. IFN-alpha2a induces IP-10/CXCL10 and MIG/CXCL9 production in monocyte-derived dendritic cells and enhances their capacity to attract and stimulate CD8+ effector T cells. J Leukoc Biol. 2002; 71:669–76. [PubMed: 11927654]

32. Sharma S, Yang SC, Zhu L, et al. Tumor cyclooxygenase-2/prostaglandin E2-dependent promotion of FOXP3 expression and CD4+ CD25+ T regulatory cell activities in lung cancer. Cancer Res. 2005; 65:5211–20. [PubMed: 15958566]

33. Jordan JT, Sun W, Hussain SF, DeAngulo G, Prabhu SS, Heimberger AB. Preferential migration of regulatory T cells mediated by glioma-secreted chemokines can be blocked with chemotherapy. Cancer Immunol Immunother. 2008; 57:123–31. [PubMed: 17522861]

34. Purow B, Schiff D. Advances in the genetics of glioblastoma: are we reaching critical mass? Nat Rev Neurol. 2009; 5:419–26. [PubMed: 19597514]

35. Schwartzbaum J, Ahlbom A, Malmer B, et al. Polymorphisms associated with asthma are inversely related to glioblastoma multiforme. Cancer Res. 2005; 65:6459–65. [PubMed: 16024651]

36. Wrensch M, Wiencke JK, Wiemels J, et al. Serum IgE, tumor epidermal growth factor receptor expression, and inherited polymorphisms associated with glioma survival. Cancer Res. 2006; 66:4531–41. [PubMed: 16618782]

37. Scheurer ME, Amirian E, Cao Y, et al. Polymorphisms in the interleukin-4 receptor gene are associated with better survival in patients with glioblastoma. Clin Cancer Res. 2008; 14:6640–6. [PubMed: 18927306]

38. Rodero M, Marie Y, Coudert M, et al. Polymorphism in the microglial cell-mobilizing CX3CR1 gene is associated with survival in patients with glioblastoma. J Clin Oncol. 2008; 26:5957–64. [PubMed: 19001328]

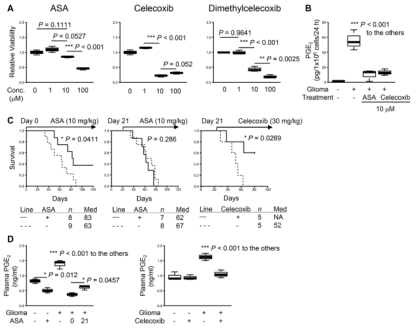

**Figure 1. Effects of NSAIDs on glioma development**

Gliomas were induced in neonatal C57BL/6 mice by intraventricular transfection of the following plasmids: *pT2/C-Luc//PGK-SB1.3* (0.2 μg), *pT/CAG-NRas* (0.4 μg), and *pT/shp53* (0.4 μg). **A,** glioma cell lines were established from WT mice and treated *in vitro* with the following NSAIDs at indicated concentrations: ASA (left), celecoxib (center), and dimethylcelecoxib (right). The cells were incubated for 24 h, and WST-1 assay was performed for cell viability. Untreated cells were used as a control. **B,** supernatants were collected from **A** to perform ELISA for $PGE_2$ levels. **C**, mice with developing tumors received daily treatment of ASA (left and center) or celecoxib (right) with indicated doses by oral gavage or through drinking water initiated on indicated days. Symptom-free survival was monitored. *P*-values are based on log-rank test. “Med” in the tables stands for median survival. **D,** plasma samples were collected from these mice at days 50 to 60 to perform ELISA for systemic $PGE_2$ levels. Numbers in the “ASA” section represent the days the treatment was initiated. **A**, **B**, and **D**, lines within boxes denote means; box upper and lower bounds indicate SD; whiskers indicate minimum and maximum values. *P*-values are based on Holm’s post hoc test.

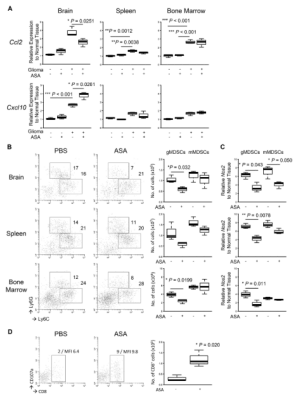

**Figure 2. Effects of ASA on glioma microenvironment**

Gliomas were induced and treated with ASA or control PBS initiated on day 0 in WT mice as described in Fig. 1. The mice were sacrificed when similar tumor size was observed by BLI at days around 50 to 60. **A**, indicated organs were collected from each mouse (3 mice/group), and total RNA was extracted to perform quantitative RT-PCR for mRNA expression levels of *Ccl2* (top) and *Cxcl10* (bottom). **B,** leukocytes were isolated from each organ to perform flow cytometry for $Ly6G^{hi}Ly6C^{lo}$ granulocytic MDSCs (gMDSCs) and $Ly6G^{-}Ly6C^{hi}$ monocytic MDSCs (mMDSCs). Representative flow data (left) and cumulative enumerations from multiple experiments (right) are shown. Numbers in the left panels indicate percentage of gated subpopulations in leukocyte-gated populations. **C**, both MDSC subpopulations were sorted, and total RNA was extracted to perform quantitative RT-PCR for mRNA expression levels of *Nos2*. **D**, the brain-infiltrating leukocytes (BILs) isolated in **B** were analyzed by flow cytometry for $CD8^{+}CD107a^{+}$ cells. Representative flow data (left) and cumulative enumerations for $CD8^{+}$ cells from multiple experiments (right) are shown. Numbers in dot plots indicate percentage of gated subpopulations in leukocyte-gated populations and MFI of CD107a on CD8-gated subpopulation.

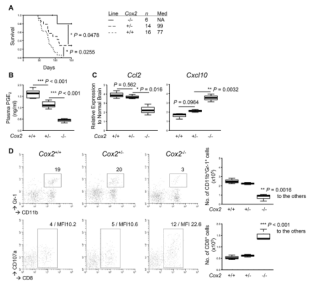

**Figure 3. Deletion of *Cox-2* alleles leads to similar effects to those by the ASA treatment**

Gliomas were induced in C57BL/6-background *Cox-2*$^{-/-}$, *Cox-2*$^{+/-}$, and *Cox-2*$^{+/+}$ mice. **A,** symptom-free survival was monitored. **B,** plasma samples were collected as described in Fig. 1 to perform ELISA for systemic $PGE_2$ levels. **C,** total RNA was extracted from the mouse brains as described in Fig. 2 to perform quantitative RT-PCR for mRNA expression levels of *Ccl2* (left) and *Cxcl10* (right). **D,** BILs were isolated to perform flow cytometry for subpopulations of $CD11b^+Gr\text{-}1^+$ (upper) and $CD8^+CD107a^+$ (lower) cells. Representative flow data (left) and cumulative enumerations from multiple experiments (right) are shown. Numbers in dot plots indicate percentage of gated subpopulations in leukocyte-gated populations; MFI of CD107a on CD8-gated subpopulation is also indicated in the bottom panels.

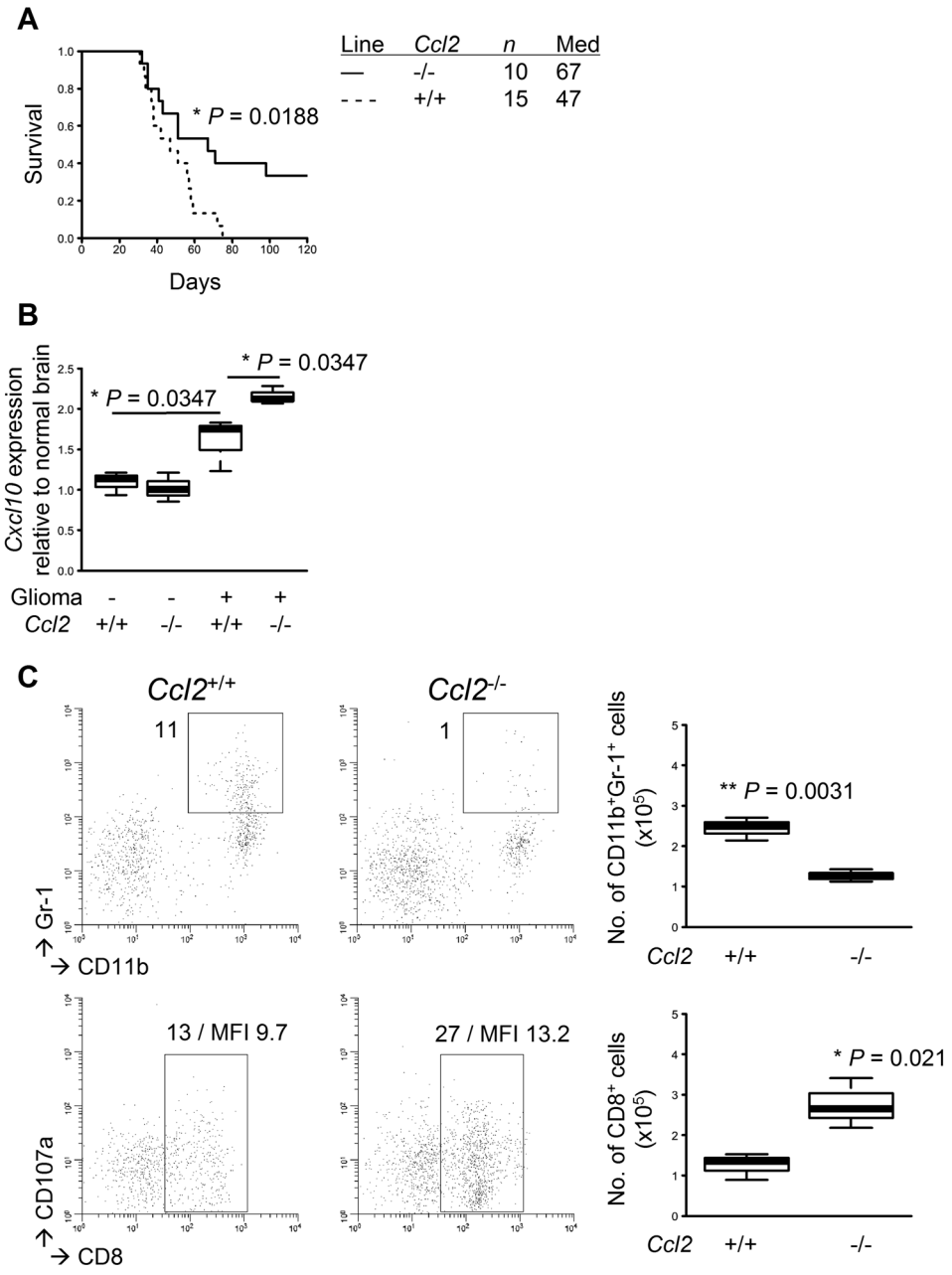


**Figure 4. Endogenous CCL2 promotes glioma development and tumor-infiltration of MDSCs**

Gliomas were induced in C57BL/6-background *Ccl2*-deficient or WT mice. **A,** symptom-free survival was monitored. **B,** total RNA was extracted from the mouse brains with or without gliomas to perform quantitative RT-PCR for *Cxcl10* mRNA expression levels. **C,** BILs were isolated to perform flow cytometry for subpopulations of $CD11b^+Gr\text{-}1^+$ (upper) and $CD8^+CD107a^+$ (lower) cells. Representative flow data (left) and cumulative enumerations from multiple experiments (right) are shown. Numbers in dot plots indicate percentage of gated subpopulations in leukocyte-gated populations; MFI of CD107a on CD8-gated subpopulation is also indicated in the bottom panels.

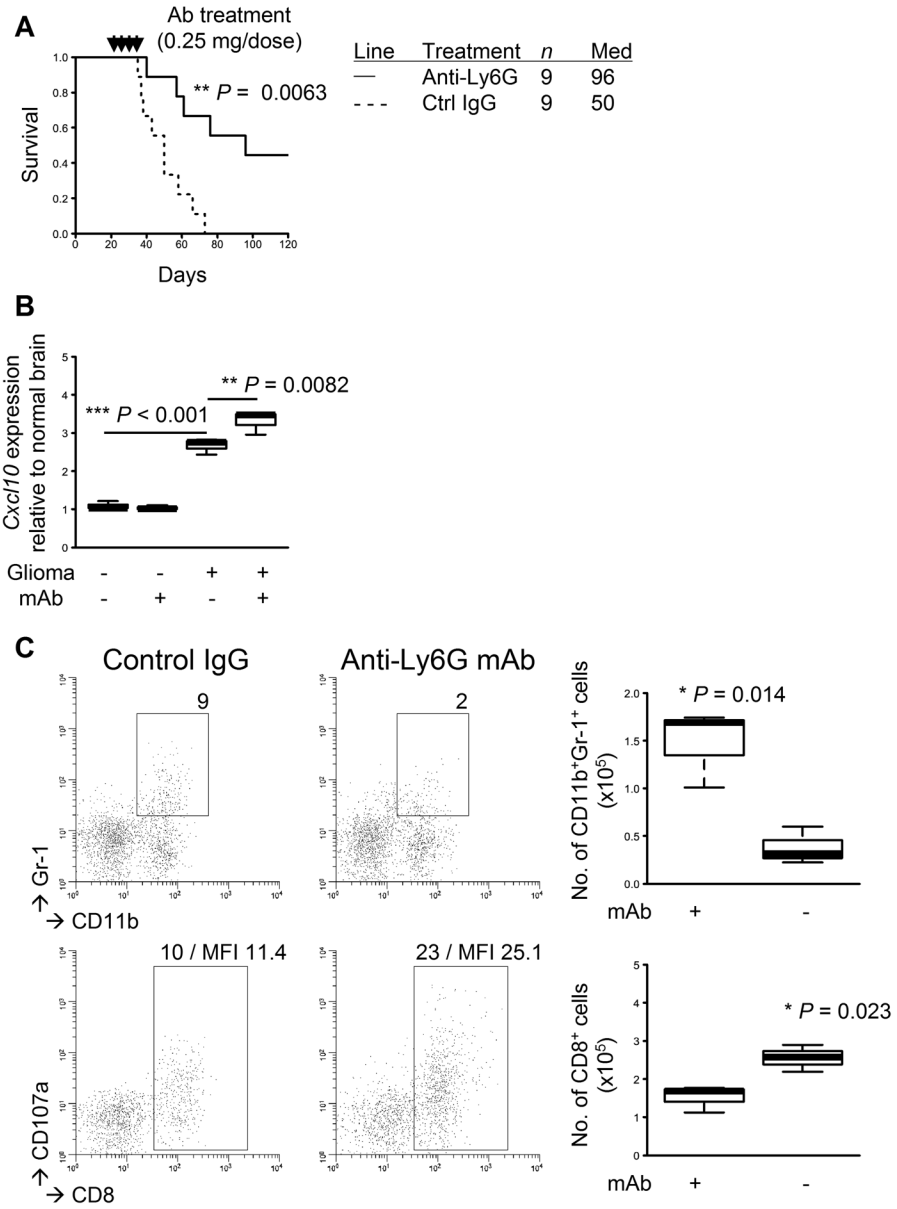


**Figure 5. mAb-mediated depletion of Gr-1$^+$ cells inhibits the glioma development**

Gliomas were induced in C57BL/6 WT mice. The mice with developing gliomas received i.p. injections of anti-Gr-1 mAb (RB6-8C5; 0.25 mg/dose) or control IgG on days 21, 23, 25, and 27 after tumor induction. **A,** symptom-free survival was monitored. **B,** total RNA was extracted from the mouse brains to perform quantitative RT-PCR for *Cxcl10* mRNA expression levels. **C,** BILs were isolated to perform flow cytometry for subpopulations of CD11b$^+$Gr-1$^+$ (upper) and CD8$^+$ (lower) cells. Representative flow data (left) and cumulative enumerations from multiple experiments (right) are shown. Numbers in dot plots indicate percentage of gated subpopulations in leukocyte-gated populations; MFI of CD107a on CD8-gated subpopulation is indicated in the bottom panels.

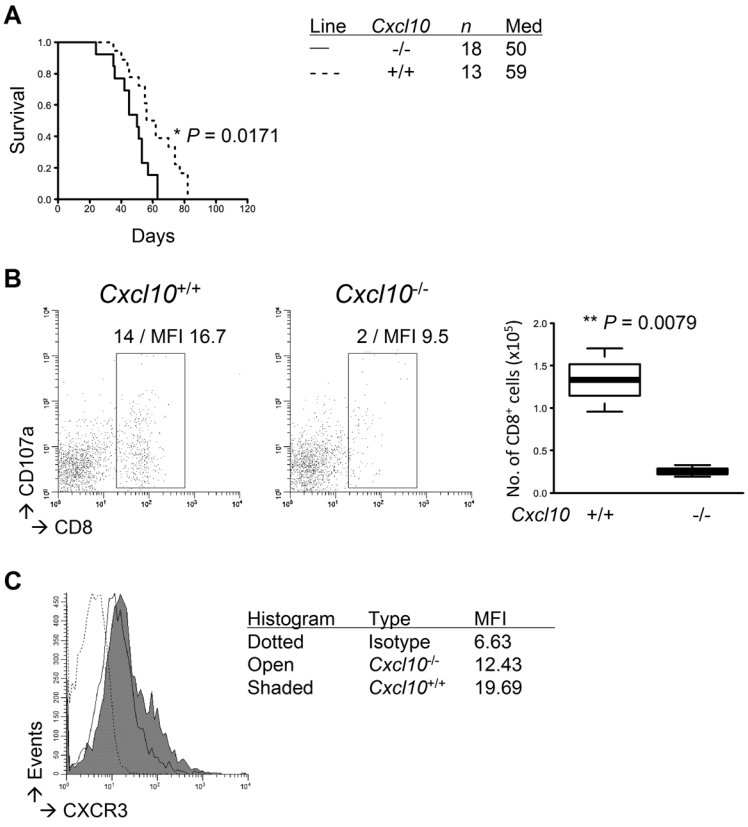


**Figure 6. Endogenous CXCL10 inhibits glioma development and promotes tumor-infiltration of CD8$^+$ T-cells**

Gliomas were induced in C57BL/6-background *Cxcl10*-deficient or WT mice. **A,** symptom-free survival was monitored. **B** and **C,** BILs were isolated to perform flow cytometric evaluation of the following molecules on CD8$^+$ subpopulations: CXCR3 (**B**) and CD107a (**C**). **C**, representative flow data (left) and cumulative enumerations from multiple experiments (right) are shown. The left panels also indicate percentage of gated subpopulations in leukocyte-gated populations and MFI of CD107a on CD8-gated subpopulation.